MATEC Web of Conferences **1**, 03001 (2012)
DOI: 10.1051/matecconf/20120103001

Experimental Identification of Concentrated Nonlinearity in Aeroelastic System

Abdessattar Abdelkefi[1], Rui Vasconcellos[2], Muhammad R Hajj[1,a], and Ali H Nayfeh[1]
[1] Department of Engineering Science and Mechanics, MC 0219, Virginia Polytechnic Institute and State University, Blacksburg, Virginia 24061, USA.
[2] Laboratory of Aeroelasticity, University of São Paulo, São Carlos, Brazil.

Abstract. Identification of concentrated nonlinearity in the torsional spring of an aeroelastic system is performed. This system consists of a rigid airfoil that is supported by a linear spring in the plunge motion and a nonlinear spring in the pitch motion. Quadratic and cubic nonlinearities in the pitch moment are introduced to model the concentrated nonlinearity. The representation of the aerodynamic loads by the Duhamel formulation yielded accurate values for the flutter speed and frequency. The results show that the use of the Duhamel formulation to represent the aerodynamic loads yields excellent agreement between the experimental data and the numerical predictions.

1 Introduction

Nonlinearities in aeroelastic systems can affect the response of aerospace vehicles and lead to complex phenomena such as flutter, limit-cycle oscillations (LCOs), chaos and bifurcations [1–3]. Such phenomena are associated with nonlinear aerodynamic or structural conditions that characterize aeroelastic systems. Regarding structural nonlinearities, they can arise from large structural deflections and/or partial loss of structural integrity. Furthermore, the effects of aging, loose attachments, and material features could lead to undesirable and dangerous responses [4]. The combination of the structural and aerodynamic nonlinearities can lead to changes in the basic response of the system such as changing it from supercritical to subcritical responses and then catastrophic behavior can occur. As such, assessing the evolution of these inevitable behaviors through modeling and analysis of these nonlinearities is important to avoid or control these dangerous responses.

In this work, we perform a nonlinear analysis to identify the concentrated nonlinearity in the torsional spring of an airfoil section. The objective is to show how the use of a cubic nonlinearity to model the concentrated nonlinearity and the Duhamel formulation to represent the aerodynamic loads can yield relevant characterization of the aeroelastic system.

2 Experimental setup of the aeroelastic system

The aeroelastic tests were carried out using an open-circuit wind tunnel with 520 mm × 515 mm of test section and its maximum air velocity of approximately 30 m/s. The experimental apparatus has been designed to characterize the aeroelastic response of an airfoil section. Based on the experimental setup, the airfoil is assumed to be two-dimensional and all parameters are defined per unit span and are assumed to be uniformly distributed. The airfoil is composed of an aluminum rigid wing that is mounted vertically at the 1/4 of the chord from leading edge by using an aluminum shaft. At the edges, the shaft is connected through bearings to the support of the plunge mechanism that includes a bi-cantilever beam made of two steel leaf-springs. Pictures of the experimental setup and of the pitch spring mechanism are presented in Figs 1 and 2, respectively.

Fig. 1. Experimental setup.

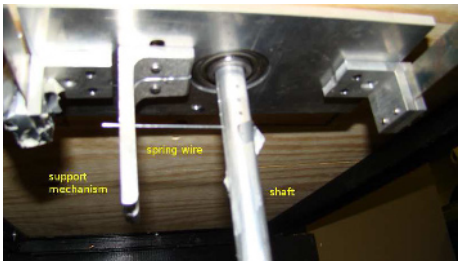

Fig. 2. Pitch spring mechanism.

[a] e-mail: mhajj@vt.edu

Table 1. Concentrated typical section parameters of the aeroelastic wing

span	Wing span (m)	0.6
b	Wing semi-chord (m)	0.0325
ρ_p	Air density (kg/m^3)	1.204
m_w	Mass of the wing (kg)	1.0662
m_T	Mass of wing and supports (kg)	3.836
I_α	Moment of inertia (kg m^2)	0.0004438
c_α	Pitch damping coefficient (kg m^2/s)	0.0115
c_h	Plunge damping coefficient (kg/s)	0.011
$k_{\alpha 0}$	Stiffness in pitch (N m)	0.942
k_h	Stiffness in plunge (N/m)	895.10

Signals of the rotational motion of the elastic axis were collected using an encoder. An accelerometer was used to collect the plunge motion. To induce motions of the wing, an initial displacement in the plunge was applied. This process was repeated starting with low speeds of about 8 m/s. It was observed that all disturbances with the same set of initial displacement would damp at speeds less than 10.9 m/s. Above this speed, limit cycle oscillations (LCO) were observed.

3 Modeling of the aeroelastic system

We model the rigid airfoil as an aeroelastic system that is allowed to move with two degrees of freedom namely the, plunge (h) and pitch (α) motions as shown in Fig. 3. The equations of motion governing this system are given by [5, 6], and are written in the following form

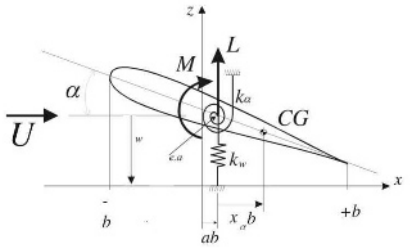

Fig. 3. Schematic of an aeroelastic system under uniform airflow.

$$\begin{bmatrix} m_T & m_w x_\alpha b \\ m_w x_\alpha b & I_\alpha \end{bmatrix} \begin{bmatrix} \ddot{h} \\ \ddot{\alpha} \end{bmatrix} + \begin{bmatrix} c_h & 0 \\ 0 & c_\alpha \end{bmatrix} \begin{bmatrix} \dot{h} \\ \dot{\alpha} \end{bmatrix} + \begin{bmatrix} k_h & 0 \\ 0 & k_\alpha(\alpha) \end{bmatrix} \begin{bmatrix} h \\ \alpha \end{bmatrix} = \begin{bmatrix} L \\ M \end{bmatrix} \quad (1)$$

In the above equations, m_T is the total mass of the wing with its support structure, m_w is the wing mass alone, I_α is the mass moment of inertia about the elastic axis, b is the semichord length, x_α is the nondimensional distance between the center of mass and the elastic axis. Viscous damping forces are described through the coefficients c_h and c_α for plunge and pitch motions, respectively. Table 1 gives values of the typical section parameters used in the analytical part. In addition, L and M are the aerodynamic lift and moment about the elastic axis. The two spring forces for plunge and pitch motions are represented by k_h and k_α, respectively. In this setup, the sole source of nonlinearity is the concentrated pitch nonlinearity. For the analysis, this nonlinearity is modeled by quadratic and cubic terms in the torsional spring, i.e, we write

$$k_\alpha(\alpha) = k_{\alpha 0} + + k_{\alpha 1}\alpha + k_{\alpha 2}\alpha^2 \quad (2)$$

4 Aerodynamic loads representation

The lift and moment as derived by Theodorsen [7] in incompressible flow are given by

$$L = -\pi\rho b^2 \left[\ddot{h} + U\dot{\alpha} - ba\ddot{\alpha}\right] - 2\pi\rho UbQC(k) \quad (3)$$

and

$$M_\alpha = \pi\rho b^2 \left[ba\ddot{h} - Ub\left(\frac{1}{2} - a\right)\dot{\alpha} - b^2\left(\frac{1}{8} + a^2\right)\ddot{\alpha}\right] + 2\pi\rho b^2 U(a+\frac{1}{2})QC(k) \quad (4)$$

where

$$Q = U\alpha + \dot{h} + \dot{\alpha}b\left(\frac{1}{2} - a\right) \quad (5)$$

and $k = \frac{wb}{U}$ is the reduced frequency of the harmonic oscillations. Clearly, the aerodynamic loads are dependent on Theodorsen's function $C(k)$. The exact expression of $C(k)$ is given by [5]

$$C(k) = F(k) + iG(k) \quad (6)$$

where F and G are functions of the Hankel and modified Bessel functions.

4.1 Duhamel formulation

Considering a simple harmonic assumption in the system's variables [8], the aerodynamic loads can be determined for arbitrary time dependent motion as [8]:

$$L = -\pi\rho b^2 \left[\ddot{h} + U\dot{\alpha} - ba\ddot{\alpha}\right] - 2\pi\rho Ub \int_{-\infty}^{+\infty} C(k) f(\omega) e^{i\omega t} d\omega \quad (7)$$

and

$$M_\alpha = \pi\rho b^2 \left[ba\ddot{h} - Ub\left(\frac{1}{2} - a\right)\dot{\alpha} - b^2\left(\frac{1}{8} + a^2\right)\ddot{\alpha}\right] + 2\pi\rho b^2 U(a + \frac{1}{2}) \int_{-\infty}^{+\infty} C(k) f(\omega) e^{i\omega t} d\omega \quad (8)$$

where

$$f(\omega) = \int_{-\infty}^{+\infty} Q(t) e^{-i\omega t} dt \quad (9)$$

Using the Wagner function as an inditial admittance and Duhamel's superposition integral, the circulatory term can be written as [8]:

$$L_c = \int_{-\infty}^{+\infty} C(k) f(\omega) e^{i\omega t} d\omega = Q(0)\phi(\tau) + \int_0^\tau \frac{\partial Q(\sigma)}{\partial \sigma} \phi(\tau - \sigma) d\sigma \quad (10)$$

where

$$Q(t) = U\alpha + \dot{h} + b\left(\frac{1}{2} - a\right)\dot{\alpha} \quad (11)$$

and $\phi(\tau)$ is Wagner function. The Sears approximation to $\phi(\tau)$ is given by [8]

$$\phi(\tau) \approx c_0 - c_1 e^{-c_2\tau} - c_3 e^{-c_4\tau} \tag{12}$$

where $c_0 = 1$, $c_1 = 0.165$, $c_2 = 0.0455$, $c_3 = 0.335$ and $c_4 = 0.3$.

Using integration by parts, the Duhamel formulation is rewritten as follows:

$$L_c = Q(\tau)\phi(0) + \int_0^\tau Q(\sigma)\frac{\partial\phi(\tau-\sigma)}{\partial\sigma}d\sigma \tag{13}$$

Using the Pade approximation to transform the integral form into a second order ordinary differential equation [9], we write

$$L_c = (c_0 - c_1 - c_3)Q(t) + c_2c_4(c_1+c_3)(\frac{U^2}{b})\bar{x} + (c_1c_2 + c_3c_4)U\dot{\bar{x}} \tag{14}$$

where $\bar{x}$ and $\dot{\bar{x}}$ are two augmented variables in the state space used to model the wake effects. The lift and moment expressions are then rewritten as:

$$L = -\pi\rho b^2\left[\ddot{h} + U\dot{\alpha} - ba\ddot{\alpha}\right] - 2\pi\rho Ub(c_0 - c_1 - c_3)Q \tag{15}$$
$$-2\pi\rho U^3c_2c_4(c_1+c_3)\bar{x} - 2\pi\rho U^2b(c_1c_2 + c_3c_4)\dot{\bar{x}}$$

and

$$M_\alpha = \pi\rho b^2\left[ba\ddot{h} - Ub\left(\frac{1}{2} - a\right)\dot{\alpha} - b^2\left(\frac{1}{8} + a^2\right)\ddot{\alpha}\right] + 2\pi\rho b^2U(16)$$
$$(a + \frac{1}{2})(c_0 - c_1 - c_3)Q + 2\pi\rho bU^3(a + \frac{1}{2})c_2c_4(c_1 + c_3)\bar{x}$$
$$+2\pi\rho b^2U^2(a + \frac{1}{2})(c_1c_2 + c_3c_4)\dot{\bar{x}}$$

On the other hand, to consider the effects of the wake dynamics of the airfoil, the augmented state variables are related to the other system parameters through the following differential equation [9]

$$\ddot{\bar{x}} = -c_2c_4\frac{U^2}{b^2}\bar{x} - (c_2 + c_4)\frac{U}{b}\dot{\bar{x}} + \frac{U}{b}\alpha + (\frac{1}{2} - a)\dot{\alpha} + \frac{\dot{h}}{b} \tag{17}$$

Substituting the expressions of the lift and moment in equation 1, the general form of the equations of motion is then written as:

$$M_1\ddot{p} + C_1\dot{p} + K_1p + Q_1(p,p) + N_1(p,p,p) = 0 \tag{18}$$

where

$$p = \begin{bmatrix} h \\ \alpha \\ \bar{x} \end{bmatrix} \tag{19}$$

$$Q_1 = \begin{bmatrix} 0 \\ k_{\alpha1}\alpha^2 \\ 0 \end{bmatrix} \tag{20}$$

and

$$N_1 = \begin{bmatrix} 0 \\ k_{\alpha2}\alpha^3 \\ 0 \end{bmatrix} \tag{21}$$

Multiplying equation (18) from the left with the inverse M_1^{-1} of M_1, we obtain

$$\ddot{p} = C_1^*\dot{p} + K_1^*p - M_1^{-1}Q_1(p,p) - M_1^{-1}N_1(p,p,p) \tag{22}$$

where $C_1^* = -M_1^{-1}C_1$ and $K_1^* = -M_1^{-1}K_1$.

In state space form, we define

$$Z = \begin{bmatrix} Z_1 \\ Z_2 \\ Z_3 \\ Z_4 \\ Z_5 \\ Z_6 \end{bmatrix} = \begin{bmatrix} h \\ \dot{h} \\ \alpha \\ \dot{\alpha} \\ \bar{x} \\ \dot{\bar{x}} \end{bmatrix} \tag{23}$$

Using these variables, equation (22) is rewritten as:

$$\begin{bmatrix} \dot{Z}_2 \\ \dot{Z}_4 \\ \dot{Z}_6 \end{bmatrix} = C_1^*\begin{bmatrix} Z_2 \\ Z_4 \\ Z_6 \end{bmatrix} + K_1^*\begin{bmatrix} Z_1 \\ Z_3 \\ Z_5 \end{bmatrix} - M_1^{-1}\begin{bmatrix} 0 \\ k_{\alpha1}X_3^2 \\ 0 \end{bmatrix} - M_1^{-1}\begin{bmatrix} 0 \\ k_{\alpha2}X_3^3 \\ 0 \end{bmatrix} \tag{24}$$

Additionally, we have:

$$\begin{aligned} \dot{Z}_1 &= Z_2 \\ \dot{Z}_3 &= Z_4 \\ \dot{Z}_5 &= Z_6 \end{aligned} \tag{25}$$

Combining these equations, we obtain the following form

$$\dot{Z} = B_1(U)Z + N_{1q}(Z,Z,Z) + N_{1c}(Z,Z,Z) \tag{26}$$

where $N_{1q}(Z,Z)$ and $N_{1c}(Z,Z,Z)$ are the quadratic and cubic vector functions of the state variables which describe the structural nonlinearity

$$N_{1q} = \begin{bmatrix} 0 \\ N_{1q2} \\ 0 \\ N_{1q4} \\ 0 \\ 0 \end{bmatrix} \tag{27}$$

$$N_{1c} = \begin{bmatrix} 0 \\ N_{1c2} \\ 0 \\ N_{1c4} \\ 0 \\ 0 \end{bmatrix} \tag{28}$$

and

$$B_1(U) = \begin{bmatrix} 0 & 1 & 0 & 0 & 0 & 0 \\ K_{111}^* & C_{111}^* & K_{112}^* & C_{112}^* & K_{113}^* & C_{113}^* \\ 0 & 0 & 0 & 1 & 0 & 0 \\ K_{121}^* & C_{121}^* & K_{122}^* & C_{122}^* & K_{123}^* & C_{123}^* \\ 0 & 0 & 0 & 0 & 0 & 1 \\ K_{131}^* & C_{131}^* & K_{132}^* & C_{132}^* & K_{133}^* & C_{133}^* \end{bmatrix}$$

where K_1^* depends on U, U^2 and U^3 and C_1^* depends on U and U^2. The matrix $B_1(U)$ has a set of six eigenvalues λ_i, $i = 1, 2..., 6$. The first four eigenvalues are complex conjugates ($\lambda_2 = \overline{\lambda_1}$, $\lambda_4 = \overline{\lambda_3}$) which are directly related to the pitch α and plunge h motions. The real parts of these eigenvalues correspond to the damping coefficients and the imaginary parts are the coupled frequencies of the aeroelastic system. The other eigenvalues λ_5 and λ_6 are related to the augmented state variable $\bar{x}$ which are negative. The solution of the linear part is asymptotically stable if the real parts of the λ_i are negative. In addition, if one of the real parts is positive, the linearized system is unstable. The speed at which one or more eigenvalues have zero real parts, corresponds to the onset of the linear instability and is termed as the flutter speed, U_f.

5 Linear analysis: Validation of the aerodynamic model

The variation of the damping term as a function of the freestream velocity when using the Duhamel formulation are presented in Fig. 4. This plot was obtained using the parameters values in Table 1. The results show analytical value of 10.90 m/s for the flutter speed. Clearly, the predicted flutter speed based on the Duhamel formulation is very close to the measured values between 10.89 m/s and 10.92 m/s. Values of the flutter frequency as predicted from the linear analysis is shown in the second column of Table 2. The corresponding experimental values are presented in the third column of Table 2. The results show that the predicted flutter frequency when considering the Duhamel formulation have a very good agreement with the experimental results.

Table 2. Comparison between theoretical and experimental results

	Duhamel formulation	Experimental results
Flutter frequency (Hz)	2.59	2.63
U_f(m/s)	10.902	$10.89 < U_f < 10.92$

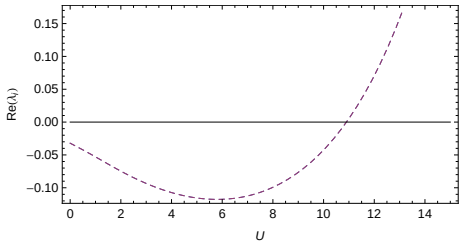

Fig. 4. Variation of the damping term as function of the freestream velocity.

6 Nonlinear analysis: Validation of the aerodynamic model and identified coefficients

The plotted curves in Figs. 5 and 6 show comparison between the experimental results and numerical integrations of the governing equations for $U = 13.68m/s$. Clearly, time histories of both the plunge and pitch motions are satisfactorily predicted by the identified parameters which are determined numerically ($k_{\alpha_1} = 3.95$ N.m and $k_{\alpha 2} = 107$ N.m).

Figs. 7 and 8 show the bifurcation diagrams for both the plunge and pitch RMS values. In these figures, a comparison is presented between numerical predictions based on Runge-Kutta method and experimental data. We note that there is a very good agreement between the experimental results and the numerical integrations. Finally, we note that the system has a supercritical behavior which is observed in the experiment.

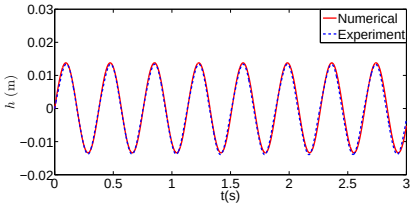

Fig. 5. Experimental and numerical time histories of the plunge motion when U=13.68.

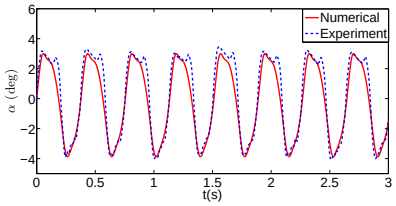

Fig. 6. Experimental and numerical time histories of the pitch motion when U=13.68.

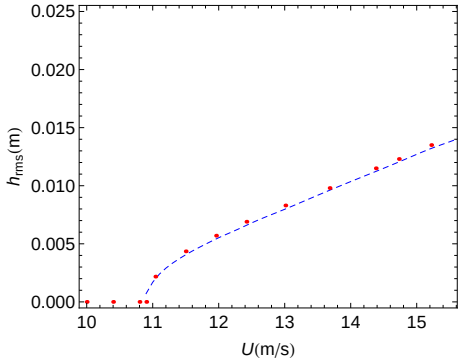

Fig. 7. Bifurcation diagram of the plunge RMS amplitude when using numerical integration (dashed lines) and experimental data (red points).

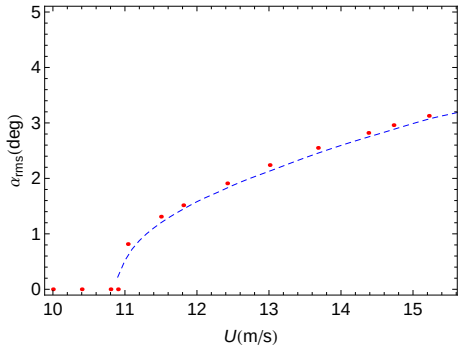

Fig. 8. Bifurcation diagram of the pitch RMS amplitude when using numerical integration (dashed lines) and experimental data (red points).

7 Conclusions

In this work, we have performed a nonlinear analysis to identify the concentrated nonlinearity in the torsional spring of a two-dimensional typical section. The concentrated nonlinearity is modeled by adding quadratic and cubic nonlinear terms in the pitch moment. We use the Duhamel formulation to model the aerodynamic loads. The results

show that using the Duhamel representation, which takes into consideration the wake effects, yield to an excellent agreement with the experimental values in both linear and nonlinear analyses.

References

1. E.H. Dowell, D. Tang, Nonlinear aeroelasticity and unsteady aerodynamics, AIAA Journal 40 1697-1707 (2002).
2. A. Abdelkefi, R. Vasconcellos, F. D. Marques, M. R. Hajj, "Modeling and identification of freeplay nonlinearity, Journal of Sound and Vibration doi:10.1016/j.jsv.2011.12.021 (2012).
3. R. Vasconcellos, A. Abdelkefi, F. D. Marques, M. R. Hajj, "Representation and analysis of control surface freeplay nonlinearity, Journal of Fluids and Structures DOI 10.1016/j.jfluidstructs.2012.02.003 (2012).
4. T. Trickey, Global and local dynamics of an aeroelastic system with a control surface freeplay nonlinearity, Duke University (2000).
5. Y.C. Fung, An introduction to the theory of aeroelasticity, Wiley NY (1955).
6. E.H. Dowell, A modern course in aeroelasticity, Kluwer, Dordrecht (1995).
7. T. Theodorsen, General theory of aerodynamic instability and the mechanism of flutter, Technical Report NACA 496 (1935).
8. R. L. Bisplinghoff, H.A. Ashley, R.L. Halfman, Aeroelasticity, Dover Publications, NY, 1996.
9. J.W. Edwards, A.H. Ashley, J.V. Breakwell, Unsteady aerodynamic modeling for arbitrary motions, AIAA Journal 17 365–374 (1979).